Engineering and Applied Science Research 2023;50(1):33-46 Research Article

Engineering and Applied Science Research

https://www.tci-thaijo.org/index.php/easr/index

Published by the Faculty of Engineering, Khon Kaen University, Thailand

New method for evaluating artificial neural network algorithm with signal detection theory and full factorial design for detecting falls

Uttapon Khawnuan*, Teppakorn Sittiwanchai and Nantakrit Yodpijit

Center for Innovation in Human Factors Engineering and Ergonomics, Department of Industrial Engineering, Faculty of Engineering, King Mongkut's University of Technology North Bangkok, Bangkok 10800, Thailand

Received 3 November 2022
Revised 12 January 2023
Accepted 24 January 2023

Abstract

Fall is one of the most critical accidents resulting in serious injuries and significant financial losses among people in all ages. This paper presents the application of full factorial design (FFD) to investigate fall detection algorithms that have multiple hyperparameters which are very difficult to identify the best values for the dataset. In this study, the algorithm factors are investigated from two motion sensors and six artifact neural network (ANN) parameters on seven possible outcomes of signal detection theory (SDT). It is found that only one accelerometer and one gyroscope and small size ANN with scaled conjugate gradient (SCG) and radial basis function (RBF) provide a higher performance classification with lower computational complexity. Experimental outcomes show the new method using statistical theory for the selection of the most effective performance of fall detection algorithm parameters. Findings from the current study could be applied to various types of classification model problems in engineering applications, such as the design of products and systems.

Keywords: Falls detection, Wearable sensor, Artifact Neural Network (ANN), Signal Detection Theory (SDT), Full factorial design (FFD)

1. Introduction

Fall accident is recognized the second major cause of unintentional injuries and deaths worldwide. Adults aged 60 years and older have the greatest number of fatal falls [1]. Falls can lead to serious quality of life problems such as hip fractures, joint sprains, or even death, and result in a financial crisis to their family and community [2]. Thus, an automatic monitoring approach for fall detection is of crucial importance for older adults and people with physical and mental disabilities [3].

During the past decades, the wearable fall detection devices are becoming generally more popular and used in many field applications due to their availability and affordable price [4]. Most wearable devices recognize falls with motion sensors such as accelerometers, gyroscopes, and magnetometers [5] by identifying the body part locations of head, trunk, and ankle [6]. In fact, the most critical part of fall detection systems is the algorithm for detecting falls and ADLs with the sensor data [7]. Detection performance relies on complexity and accuracy of threshold-based method which influences the reliability of results [8]. As such, ANN is recognized due to their ability to perform a powerful classification of pattern recognition. A prior study has revealed that ANN has a good performance in choosing the right answer and have been used for creating fall detection algorithms [9].

Sensor is a major part of fall detection wearable devices. Benefits of using wearable sensors include the ease of use, the convenience to attach the body, and the low price as compared to external sensors [10]. The characteristics of the wearable devices such as size, shape, and weight enable them to be worn easily by users [11] and depend upon characteristics of sensors.

ANN has numerous parameters. The major problem in applying ANN is the optimization of their parameters using a trial-and-error process. It usually takes a certain period of time [12] and only one factor can be studied at a time. As such, unreliable and misleading results with wrong conclusions would be found [13]. However, the trial-and-error method has been used for fall detection analysis and design in a recent study where ANN parameters are tuned manually [14].

The evaluation of system accuracy has utilized statistical techniques to assist in making decisions under various conditions of uncertainty to improve the design and the performance of algorithm [15]. For example, the SDT has been used for examining human's ability to detect a signal from noises in various situations [16] and are applied for performance improvement of fall detection algorithms [9]. Four outcomes (hit, miss, false alarm, and correct rejection) of SDT have occurred, but A' and B'' are not used for evaluating the performance of fall detection algorithms. For example, the work of Lin et al. [17] implements the FFD to explore factors affecting SDT outcomes for designing the product.

FFD is a mathematical and statistical approach which is helpful and necessary for complex simulation analysis that allows an analyst to have a better understanding of unique situations and form desired process results as needed [18]. The FFD concept can be extended to an ANN design when defining the network parameters [19, 20]. In general, the FFD is used for investigating all possible combinations of factors and levels [21], leading to more reliable outcomes in realistic circumstances. Interestingly, it has been mentioned that FFD offers the best configuration for improving the performance of ANN models [22, 23].

*Corresponding author. Tel.: +6688 753 5175
Email address: uttapon.kn@gmail.com
doi: 10.14456/easr.2023.5

In sum, motion sensor and ANN parameters are major factors for designing wearable fall detection systems [11, 24]. The objective of this study is to design the fall detection algorithm based upon FFD findings from the investigation of influencing factors (both motion sensor and ANN parameters) on SDT outcomes. The contribution of this study provides the framework by focusing on parameters that have a significant effect on the performance of classification models for selecting optimal parameters of ANN models.

2. Materials and methods

The research methodology is shown in Figure 1 where FFD and SDT principles are used to explore the effects of motion sensors (accelerometer and gyroscope) and ANN factors on SDT outcomes. The findings of this concept provide a better understanding of the effects of each parameter on ANN algorithm performance [22, 23] and analyze the optimal setting configuration [25].

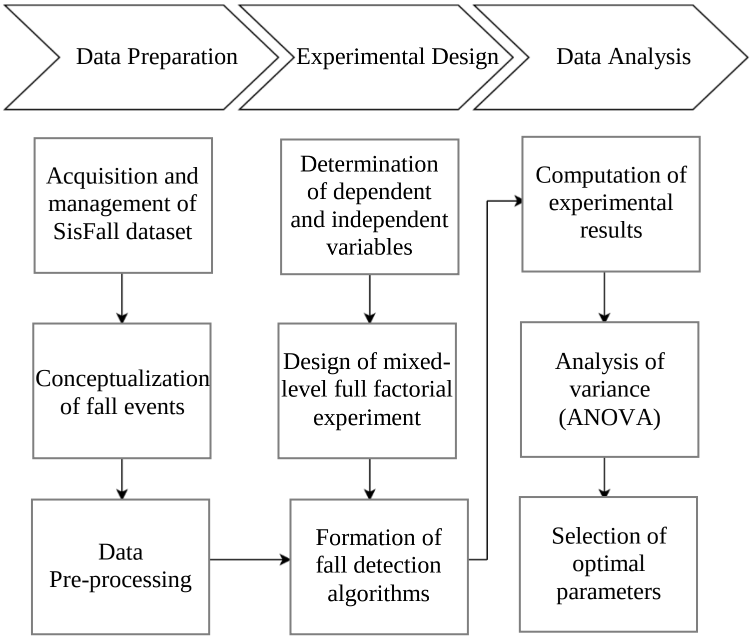

Figure 1 The research methodology

2.1 Data preparation

2.1.1 Acquisition and management of SisFall dataset

The SisFall dataset is one of the largest public datasets [26, 27] available for research projects and has been applied in previous fall detection studies [28] since it includes activities before a fall occurred or unoccurred during dangerous situations [29].

This study employs the SisFall dataset because it has the largest amount of data, both on number and heterogeneity of ADLs and subjects [30, 31]. Details of all participants and their movement characteristics obtained from a total of 38 participants (19 males and 19 females) which are divided into two age groups (adult and elderly). The adults (11 males and 12 females; ages mean = 23.39 years, standard deviation = 3.39 years) and elderly (8 males and 7 females; ages mean = 65.87 years, standard deviation = 3.78 years) have taken part in this study. The SisFall dataset consists of 19 types of ADLs and 15 types of falls found among the adult and elderly participants.

In fact, elderly people have more risk of falls when walking and trying to get up from a chair. These types of falls are included in the current study and used to investigate in the previous study [28]. Examples of falls are (1) fall forward while walking caused by a slip, (2) fall backward while walking caused by a slip, (3) lateral fall while walking caused by a slip, (4) fall forward while walking caused by a trip, (5) fall forward while jogging caused by a trip, (6) fall forward when trying to get up, etc. However, the SisFall dataset has a variety of highly dynamic ADLs (quick lie-to-bed and sit-to-stand) that could lead to many false alarms when using the threshold technique [32]. Table 1 presents details of the participants.

Table 1 The characteristics of the participants

Age Group (n)	Gender (n)	Age (yr)			Height (m.)	Weight (kg.)
		Range	Mean	SD		
Adult (23)	Male (11)	19–30	23.55	3.31	1.65–1.83	58–81
	Female (12)	19–30	23.25	3.32	1.49–1.69	42–63
Elderly (15)	Male (8)	60–71	65.75	3.20	1.63–1.71	56–102
	Female (7)	62–75	66	4.11	1.50–1.69	50–72

2.1.2 Conceptualization of fall events

Fall events are divided into four phases [33]. Firstly, the pre-fall phase describes the ADLs performed before falls. Secondly, the critical phase is just a short time that body suddenly moves toward, backward, or towards the side and impinges on the ground. Thirdly, the post-fall phase is commonly represented by a body resting on the ground with no movement after the fall has happened. Finally, the recovery phase is the time after post fall phase that the person gets up without help from another person.

2.1.3 Data pre-processing

The raw motion sensor data are segmented by the impact point-based method in the magnitude of acceleration for falls [34] and ADLs [35] with a time interval of 6 seconds [35, 36]. At a fall, the posture of body is changed and has influenced on the acceleration value as captured by motion sensors in individual axes within 2 seconds [37].

This study focuses on only the first three phases of falls (pre fall, critical, and post fall) with the impact point-based method where each phase has a same time interval of 2 seconds as presented in Figure 2. For the feature extraction, seven descriptive statistics (maximum, mean, median, smallest, most frequent, standard deviation, and variance value) of each phase are prepared and fed into the feedforward neural network (FFANN). Figure 3 (a) and (b) show examples of acceleration and angular velocity data, respectively.

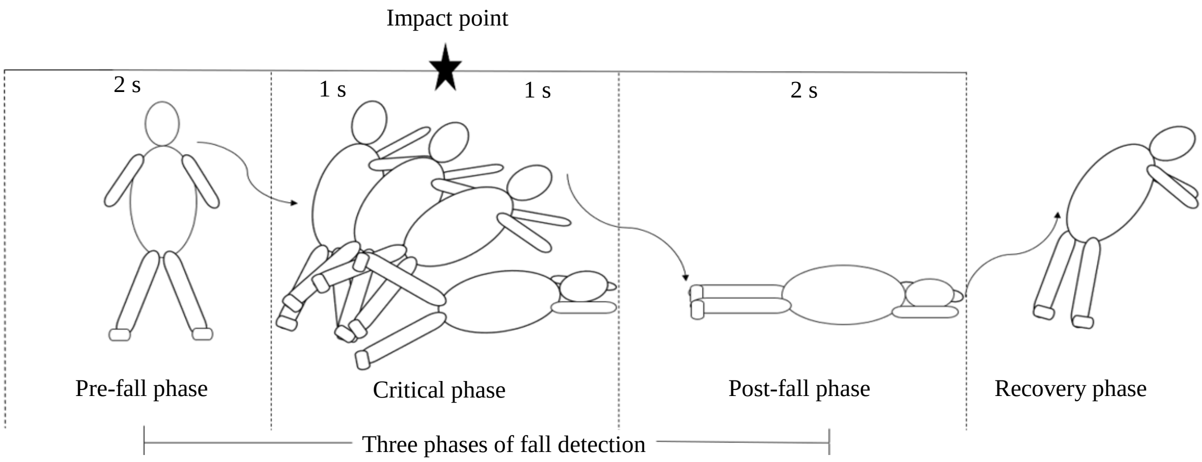

Figure 2 Four phases of falls

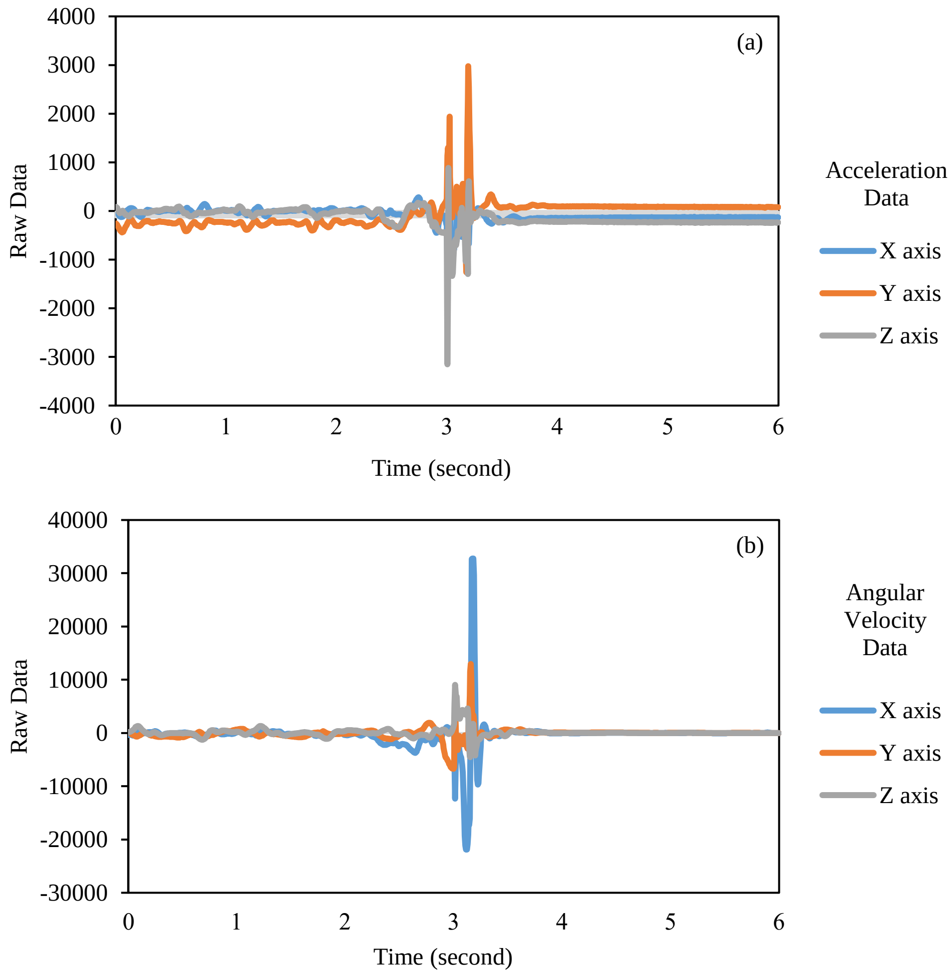

Figure 3 Examples of acceleration (a) and angular velocity (b) data from motion sensors

2.2 Experimental design

2.2.1 Determination of dependent and independent variables

2.2.1.1 Dependent variables

The seven outcomes of SDT are investigated as the hit, miss, false alarm, correct rejection, A', $B"$, and zROC plot. Examples of SDT applications have found in various categories, such as visual and audio detections [38], audio alarm systems [39], screening tool [40], hybrid inspection system [41], radial menus [42], feed-water monitoring system [43], cargo security screeners [44], and customers' creditworthiness [45]. A similar and recent study is conducted for examining baseball games with SDT and ROC space [17].

General definitions of the seven dependent variables as described in the SDT framework for fall detection system can be given as follows. Hit is determined by detecting a fall when it happens. Miss refers to a fall that has occurred, but the system does not detect it. A false alarm relates to a fall that has not occurred but it is detected. Correct rejection indicates that the system does not detect a fall when it does not exist.

Measures of nonparametric index of A' and $B"$ are most popular because they are assumed to be free from normal distribution assumptions. These indexes have been methodologically and computationally well developed by Grier (1971) and generally applied in SDT based research [44, 46].

A' can be determined by the equation (1) and generally covers the ranges from 0 to 1. For example, if A' is 0.5, it is implied that the system cannot differentiate signals from the noise. In case of A' less than 0.5, it may result from response confusion or sampling error, and if A' equals 1, it shows the perfect performance of the system.

$$A' = .5 + [sign(H-F)\frac{(H-F)^2+|H-F|}{4MAX(H,F)-4HF}] \tag{1}$$

Where .5 is a constant number. H and F refer to hit and false alarm rates, respectively. As given; if $(H-F)$ > 0 (i.e., $H > F$), sign $(H-F)$ = +1; if $H = F$, sign $(H-F)$ = 0; and otherwise (i.e., $H < F$), sign $(H-F)$ = -1; $MAX(H,F)$ equals either H or F, whichever is greater.

$B"$ is a well-known nonparametric measure concerning response bias [47] as shown in equation (2). $B"$ can cover from - 1 (severe bias in yes response approval) to 1 (severe bias in no response approval). If $B"$ = 0, it refers to no response bias.

$$B^{"} = sign(H-F)\frac{H(1-H)-F(1-F)}{H(1-H)+F(1-F)} \tag{2}$$

zROC plot draws z-score of false alarm rate on the x-axis and z-score of hit rate on the y-axis to show the mean performance in all experiments [48]. Thus, the point in the top-left corner of the zROC plot is the best possible detection, describing 100% hit and 0% false alarm probability.

2.2.1.2 Independent variables

The following independent variables are described as follows:

a) Motion sensors

Two motion sensors (accelerometer and gyroscope) are critical parts of fall detection systems. The data of three axes of the accelerometer and gyroscope (see Figure 4) are measured from the sensor's linear acceleration and angular velocity parameters concerning the gravitational characteristics. The participants' movement characteristics appeared in the SisFall dataset are collected from motion sensors at 200 Hz of wearable device attached to their waist. The sensors have consisted of an ADXL345 accelerometer (configured for ±16 g, 13 bits of analog to digital converter (ADC)), a Freescale MMA8451Q accelerometer (configured for ±8 g, 14 bits of ADC), and an ITG3200 gyroscope (±2000º/s, 16 bits of ADC, Texas Instruments, Dallas, Texas, USA).

The advantage of using both motion sensors is that one sensor compensates for limitations of another. For example, the mistake of drift from integrating gyroscope data can be corrected by the accelerometer-based orientation estimates and the mistake of orientation by earth's gravity in the accelerometer can be corrected by gyroscope-based rotation estimates [49]. The type and the number of sensors are introduced based upon the characteristics of wearable fall detection devices employed to collect motion data [31]. As such, a combination of one accelerometer and one gyroscope is set as a low level and two accelerometers and one gyroscope is set as a high level in this study.

b). Artificial neural network (ANN)

The hidden layer is found among the input and output layers. There is a specific number of neurons in all layers. Usually, the number of hidden layers is 1, 2, or 3. However, the zero layer can be found but are not being generally utilized [13] because the ANN with zero hidden layers cannot represent nonlinear separable decisions or functions [50].

Each epoch refers to one cycle of training the model through a training data set. The number of epochs allows an increase in the model's accuracy and training time. This study evaluates three levels (100, 500, and 1000) of epoch which have been used in fall detection systems [51-53].

The number of neurons in the hidden layers performs a vital role in classification. The determination of number of neuron in the hidden layers equals to K × (N+1); where N = the number of neurons in the input layer, and K=1, 1.5, 2 [13].

The learning rate is a hyperparameter or adjustable parameter to determine step size for finding the optimal solution of problems. Learning rate should be seriously taken into consideration as a high value can cause a fast convergence of algorithm but might miss an optimal solution. A low value may result in a long period of time for training process and might get stuck at a local minima. Three levels (0.1, 0.5, and 1) of learning rate are investigated in the current study [54].

The training algorithm is used to update network weights and bias values [55]. In this study, two algorithms are selected for training ANNs in all experiments. The first algorithm is a SCG which is usually found in the training process [56]. The second algorithm is a RP which has an excellent performance for training FFANN [57].

Transfer (or activation) function is recognized for the calculation of the layer outputs of data coming from the previous hidden layer. In this research, two functions are examined: the HTG [58] and the RBF [59].

2.2.1.3 Control variables

All participants have no mobility problems. The position of motion sensors is fixed with a wearable device similar to a belt buckle as shown in Figure 4. Orientation of the motion sensors displays the positive x-axis guiding to the right side of the participant, the positive y-axis in the gravity direction, and the positive z-axis in the forward direction.

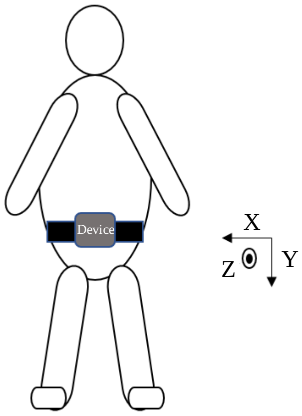

Figure 4 The orientation of motion sensors, modified from [28]

2.2.2 Design of mixed-level full factorial experiments

The current research explores the process of designing fall detection algorithm with the considerations of motion sensor and ANN characteristics using SDT and FFD principles. In addition, FFD can determine detailed insight fall detection algorithm performance with an emphasis on seven critical factors (1 motion sensor and 6 ANNs) with different levels as shown in Table 2. The evaluation of effect of seven SDT outcomes (hit, miss, false alarm, correct rejection, A' and B'', and zROC plot) is performed. A mixed-level full factorial design is conducted where all sensor and ANN factors serve as within-subject design. Three replicates are performed in each treatment which includes training and testing trials for each treatment with FFANN configuration, so there is a total of 1,944 runs in MATLAB.

Table 2 Sensor and ANN factors and levels

Factors / Level	Type and the number of sensor (A)	Hidden layer (B)	Epoch (C)	Number of neuron (D)	Learning rate (E)	Training function (F)	Transfer function (G)
(1)	1 accelerometer, 1 gyroscope	1	100	1	0.1	scaled conjugate gradient (SCG)	hyperbolic tangent sigmoid (HTG)
(2)	2 accelerometers, 1 gyroscope	2	500	1.5	0.5	resilient backpropagation (RP)	radial basis function (RBF)
(3)	-	3	1000	2	1	-	-

2.2.3 Formation of fall detection algorithms

The FFANN is classification algorithms that have been used for training and testing the SisFall dataset collected from motion sensors (acceleration and angular velocity data) attached on the waist to differentiate falls from ADLs. In FFANN, the feature extracted data feeds in only one direction moving forward from the input nodes, through the hidden nodes and to the output nodes. There are no cycles or loops in the network. The FFANN in this study is the multi-layer perceptron class where the network consists of multiple layers of neurons interconnected in forward direction. Each neuron in each layer has connected with neurons in the subsequent layer. FFANN is trained by training dataset. The testing dataset is used to test FFANN on a different person for supporting realistic evaluation [34].

2.3 Data analysis

2.3.1 Computation of experimental results

All computations are conducted on a computer equipped with Intel(R) Core(TM) i7-6700 at 3.40 GHz, 16 GB of RAM, and a GeForce GTX1060 GPU with 6 GB of memory with Minitab Version 17 software (Minitab, Inc., State College, PA, USA), and MATLAB version R2020a (Mathworks, Inc., Natick, MA, USA) for experimental design, data analysis, and ANN architectures (creating, training, and testing). The A', B', and zROC plot are calculated in Excel. The zROC plot is utilized to recognize the z-score of hit and false alarm of all experiments.

2.3.2 Analysis of variance (ANOVA)

Previous studies reveal that ANOVA is the most efficient, conceptually simple, powerful, and popular statistical analysis method for determining the optimal configuration by evaluating statistically significant factors [25, 60, 61]. Main effects and interactions of motion sensor and ANN factors are investigated by ANOVA. Fisher's least significant difference (LSD) is applied to define statistical differences in the levels of factors. Statistical analysis is performed with a 95% confidence interval ($\alpha = 0.05$) and computed by Minitab.

2.3.3 Selection of optimal parameters

The trial-and-error method is the traditional method for selecting optimal parameters. However, it causes problems such as taking a long time [12] and not focusing on the optimal solutions as expected [13, 62]. Therefore, this study uses the FFD to prove the statistical difference of parameters based on SDT outcomes for the selection of optimal parameters in the proposed fall detection algorithm.

3. Results

After manipulating mixed-level FFD with 3 replicates, leading to 1,944 runs, it has been found that a motion sensor and four of six ANNs (hidden layer, epoch, number of neuron, learning rate, training function, and transfer function) have significantly influenced seven SDT outcomes (hit, miss, false alarm, correct rejection, A', B'', and zROC) in different ways. In fact, the epoch and learning rate become noise factors and can be eliminated which has been done in the previous publication [13]. Therefore, only five crucial factors are investigated for the further study.

Another mixed-level FFD experiment on a motion sensor and four ANN factors, serving as within-subject design is conducted. The experiment is replicated three times, giving a total of 216 experimental runs. Additionally, the epoch = 100, and learning rate = 1 are fixed for having the faster training time as both of them have no significant impact on SDT outcomes. The Table 3 shows ANOVA results (F value) of significant dependent variables. Two-way and three-way interactions have tested. Interestingly, there is no significant four way and five-way interactions found among these five factors at a 95% confidence level ($p > 0.05$).

Table 3 ANOVA results of significant dependent variables

Source	**Hit/Miss**	**FA/CR**	$\boldsymbol{A'}$	$\boldsymbol{B''}$
Type and the number of sensor (A)	0.43	1.76	1.10	0.05
Hidden layer (B)	1.50	0.13	0.92	2.25
Number of neuron (D)	2.78	1.56	3.98*	1.59
Training function (F)	37.80**	8.88**	58.52**	64.43**
Transfer function (G)	13.07**	1.23	20.98**	11.66**
A*G	0.17	5.02*	1.99	0.05
B*G	3.42*	0.87	2.35	0.19
D*F	2.60	1.16	3.32*	0.94
F*G	12.14**	2.87	8.52**	36.17**
B*F*G	4.19*	0.83	2.08	2.64

*$p < 0.05$; **$p < 0.01$.
FA = false alarm; CR = correct rejection.

ANOVA results of significant dependent variables are discussed as follows:

3.1. Hit rate

The training function ($\mathrm{F} = 37.80, p < 0.01$) and transfer function ($\mathrm{F} = 13.07, p < 0.01$) have significantly different effect on the hit. However, no significant difference is found for the type and number of sensor ($\mathrm{F} = 0.43, p > 0.05$), hidden layer ($\mathrm{F} = 1.50, p > 0.05$), and the number of neurons ($\mathrm{F} = 2.78, p > 0.05$). Interactions between hidden layer and transfer function ($\mathrm{F} = 3.42, p < 0.05$), training function and transfer function ($\mathrm{F} = 12.14, p < 0.01$), and hidden layer, training function and transfer function ($\mathrm{F} = 4.19, p < 0.05$) are significant difference, as shown in Table 3.

The LSD test shows that the SCG ($\mathrm{Mean} = 0.952, p < 0.01$) has a significantly higher hit than the RP ($\mathrm{Mean} = 0.754$; $p < 0.01$) that yields network weights and bias values with higher hit for falls detection algorithm. The hit of RBF ($\mathrm{Mean} = 0.910, p < 0.01$) is significantly higher than hit of HTG ($\mathrm{Mean} = 0.794$; $p < 0.01$). Hidden layer interacts significantly with transfer function ($\mathrm{F} = 3.42, p < 0.05$). Figure 5 (a) shows that the RBF has a higher hit than the HTG in every hidden layer and can provide the proper layer outputs calculated from the previous hidden layer, leading to the improvement of fall detection algorithm. As such, the SCG with any transfer functions can detect falls with high accuracy as shown in Figure 5 (b).

The three-way interactions of hidden layer, training function, and transfer function are shown in Figure 5 (c). FFANN is trained by the SCG provide a high hit at every hidden layer and transfer function. The LSD test also indicates no significant difference of hit when SCG is used ($p > 0.05$). It can be implied that ANN with small size of hidden layers and SCG can be employed in fall detection algorithm.

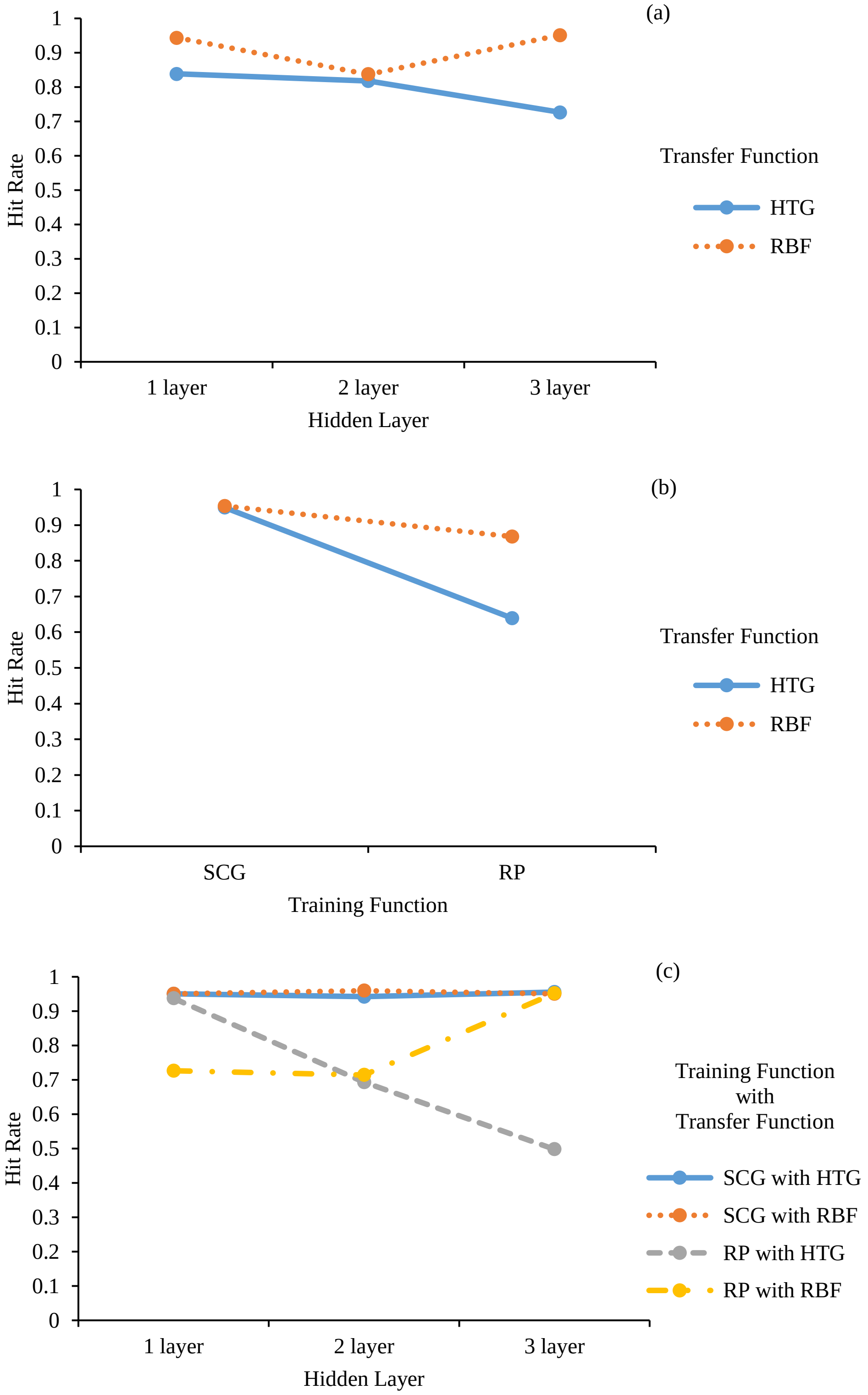

Figure 5 Interaction between hidden layer and transfer function (a), training function and transfer function (b), and hidden layer, training function and transfer function (c) for the hit rate

3.2. Miss rate

The training function ($F = 37.80, P < 0.01$) and transfer function ($F = 13.07, P < 0.01$) have significantly influenced on the miss, as shown in Table 3. The LSD test shows that the miss of the SCG ($Mean = 0.048, p < 0.01$) is significantly lower than the miss of the RP ($Mean = 0.246, p < 0.01$), and the miss of RBF ($Mean = 0.09, p < 0.01$) is significantly lower in comparison to the miss of the HTG ($Mean = 0.206; p < 0.01$), as shown in Figure 6 (a) and (b). Therefore, the SCG and the RBF produce the lowest miss in a small ANN structure. Furthermore, a three-way interaction between hidden layer, training function, and transfer function are found on the miss ($F = 4.19, p < 0.05$) as shown in Figure 6 (c), corresponding to the findings of the hit rate in Section 3.1 as the hit and miss rates are opposite indicators [17].

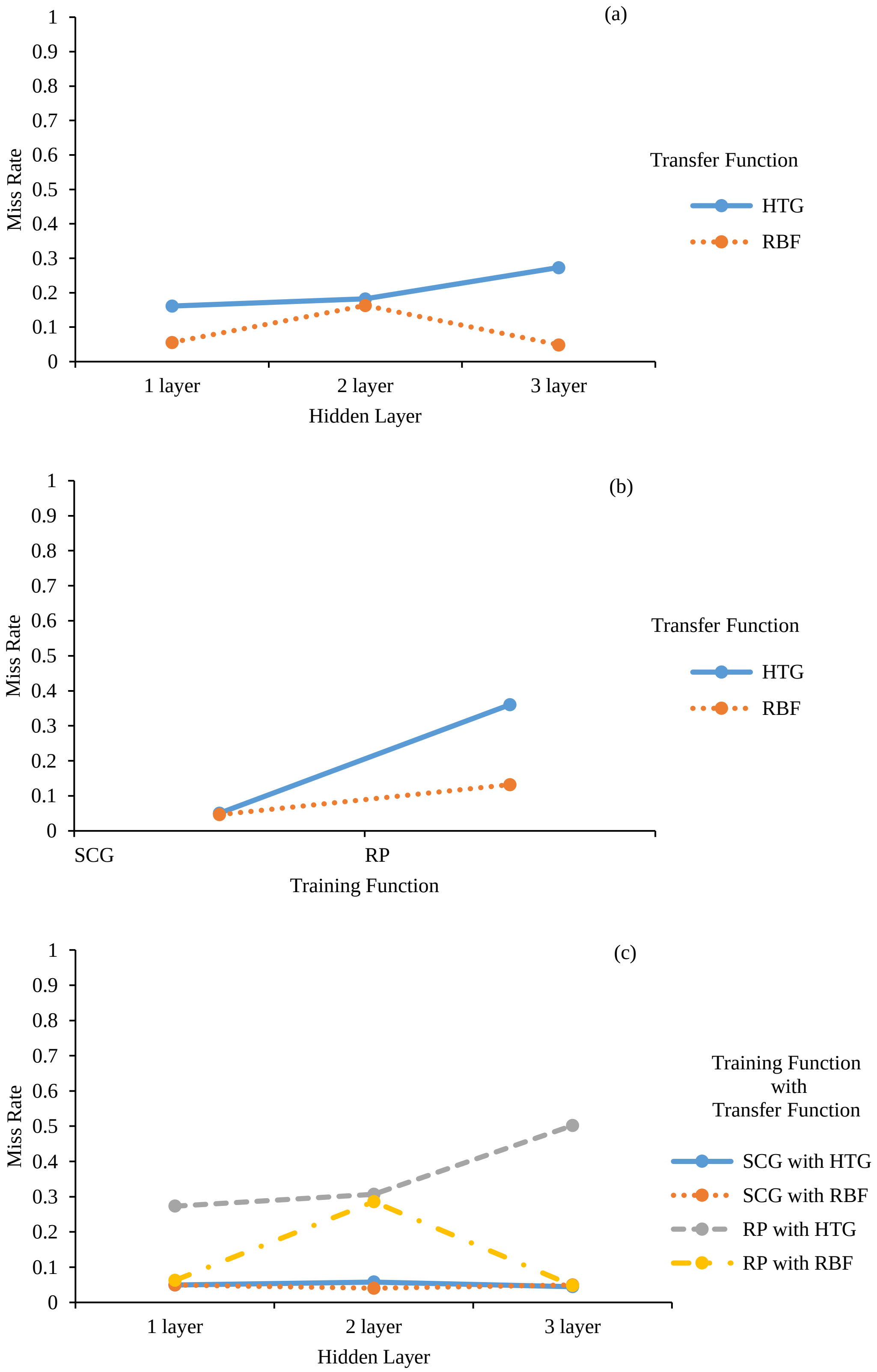

Figure 6 Interaction between hidden layer and transfer function (a), training function and transfer function (b), and hidden layer, training function and transfer function (c) for the miss rate

3.3. False alarm rate

Training function ($F = 8.88, p < 0.01$) has a significant impact on the false alarm rate, as shown in Table 3. The false alarm of the SCG ($\text{Mean} = 0.225, p < 0.01$) is significantly lower than the false alarm of the RP (Mean = 0.336, p < 0.01). The false alarm of the RBF with one accelerometer and one gyroscope, gives the lowest false alarm, as shown in Figure 7. The interaction leads to the reduction of the size, weight, memory and computational complexity of device.

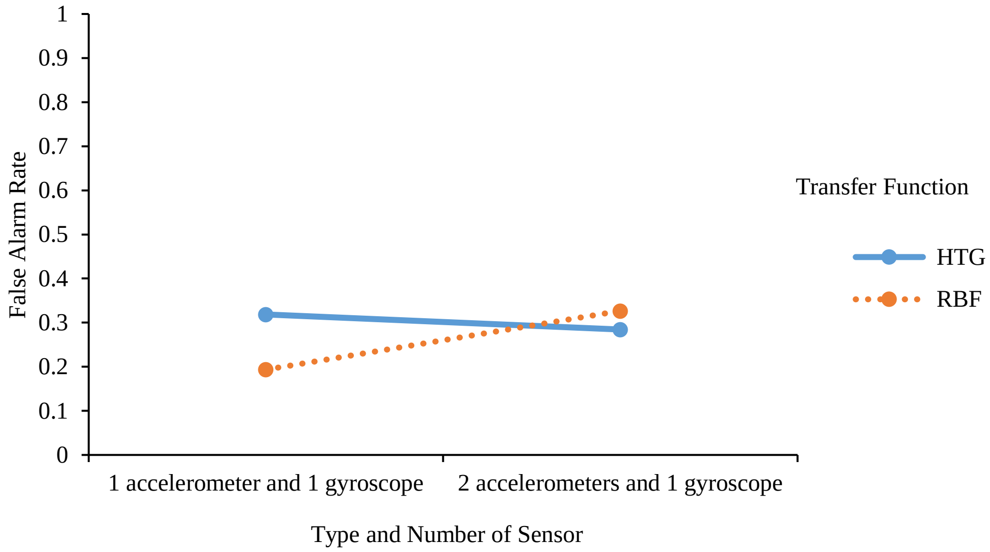

Figure 7 Interaction between type and number of sensor and transfer function for the false alarm rate

3.4. Correct rejection rate

Based upon the LSD test, the SCG allows the higher correct rejection as it (Mean = 0.775, p < 0.01) is significantly greater than the correct rejection of the RP (Mean $= 0.664; p < 0.01$). Figure 8 shows that the sensor (one accelerometer and one gyroscope) with the RBF provides the highest correct rejection. This could be implied that the fall detection algorithm can differentiate falls from ADLs.

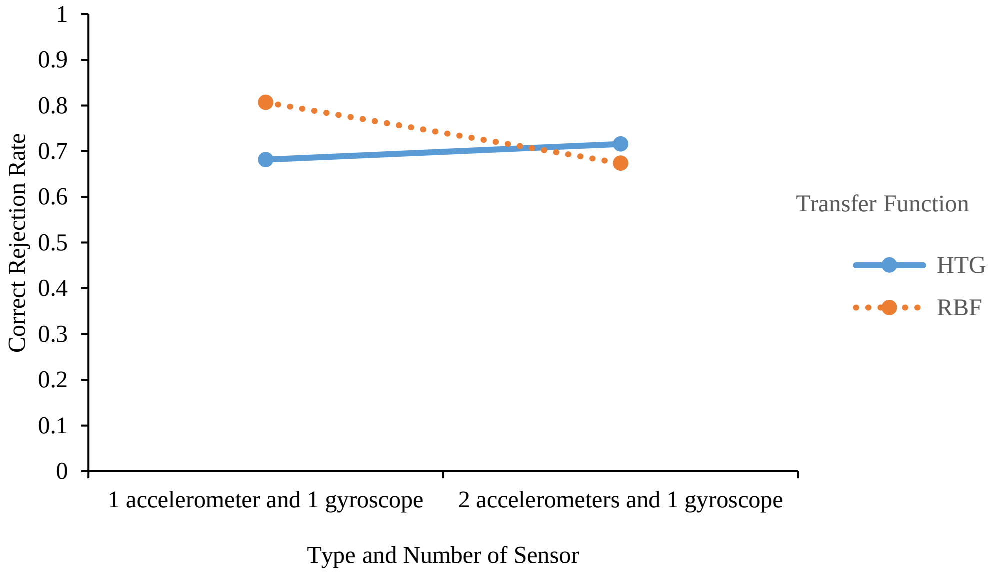

Figure 8 Interaction between type and number of sensor and transfer functions for the correct rejection rate

3.5. A'

The Shpiro-Wilk test shows that SDT outcomes of fall detection algorithm are not normally distributed (α = 0.05). Thus, the SDT d' and β are performed with nonparametric measure of (A') and (B'), and the zROC plot for the design of fall detection algorithm in FFD phase. Table 3 shows that the number of neurons ($\mathrm{F} = 3.98, p < 0.05$), training function ($\mathrm{F} = 58.52, p < 0.01$) and transfer function ($\mathrm{F} = 20.98, p < 0.01$) have a significant impact on the A'.

LSD test illustrates that the A' in the low level (K=1) number of neuron (Mean $= 0.89, p < 0.05$) is significantly higher than the A' in the middle level (K=1.5) (Mean $= 0.84, p < 0.05$) and high level (K=2) (Mean $= 0.82, p < 0.05$) number of neuron. The A' of the SCG (Mean $= 0.92, p < 0.01$) is significantly higher than the A' of the RP (Mean $= 0.77; p < 0.01$). The means of A' for the RBF and the HTG are 0.89 and 0.80, respectively. It should be noted that the design of fall detection algorithm should consider the A' with a high value for the more accurate and reliable performance. Figure 9 (a) shows that the interaction effect achieves the high hit and the low false alarm at the lowest level of the number of neurons while the RBF with the SCG provides the highest A' among the other interactions, as shown in Figure 9 (b).

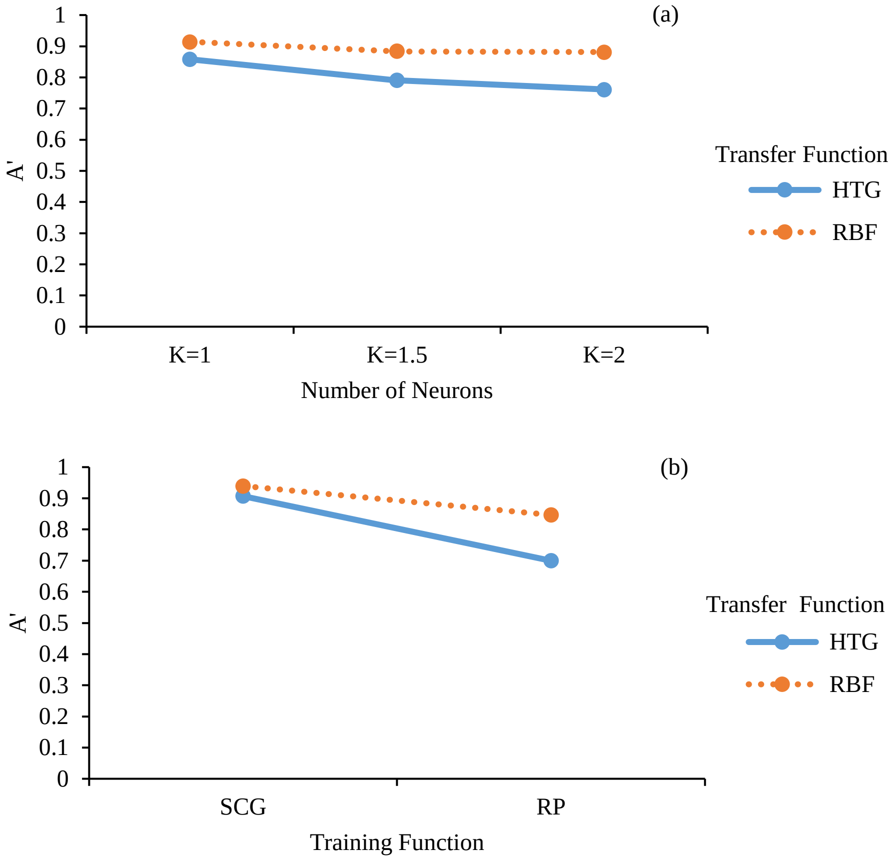

Figure 9 Interaction between the number of neurons and training function 9 (a), and training function and transfer function 9 (b) for the A'

3.6. $B"$

The significant differences on the $B"$ are found for the training function ($\mathrm{F} = 64.43, P < 0.01$) and transfer function ($\mathrm{F} = 11.66, P < 0.01$). The $B"$ is significantly lower in the SCG ($\text{Mean} = -0.54, p < 0.01$) than the RP ($\text{Mean} = -0.18, p < 0.01$). The ANN is trained by the SCG, resulting that fall detection makes more severe bias in yes response approval. The $B"$ is significantly lower for the RBF ($\text{Mean} = -0.43, p < 0.01$) than for the HTG ($\text{Mean} = -0.28, p < 0.01$).

The effects of interaction between training function and the transfer function are observed from the plot as the $B"$ is minimum with the use of the HTG and the SCG, as illustrated in Figure 10. The fall detection algorithm produces mostly *yes* responses on signal and noise trials. It is meant that the interaction produces a high hit and false alarm for the classification between falls and ADLs.

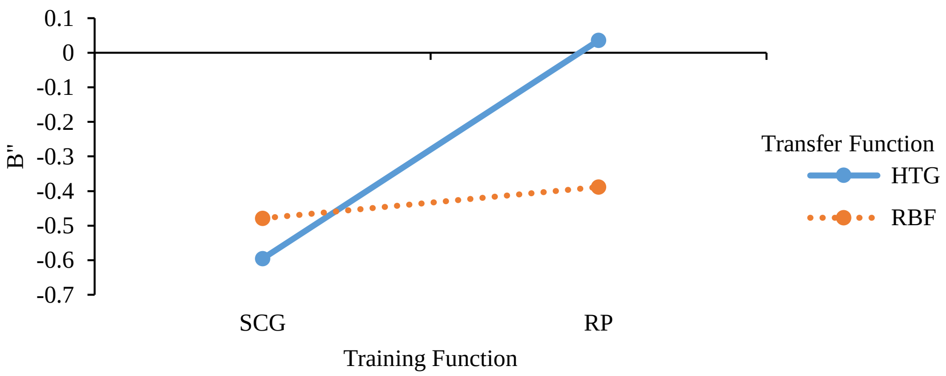

Figure 10 Interaction plot between the training function and transfer function for the $B"$

3.7. zROC plots

Figure 11 illustrates the zROC plot of 216 experimental runs by plotting in two coordinates (z-score of false alarm and hit rates). It reveals the prediction point of experimental runs appears at the top left of the second quadrant as the highest prediction accuracy and highest fall detection performance with lowest false alarm rate, indicating the most accurate and reliable performance for detecting falls.

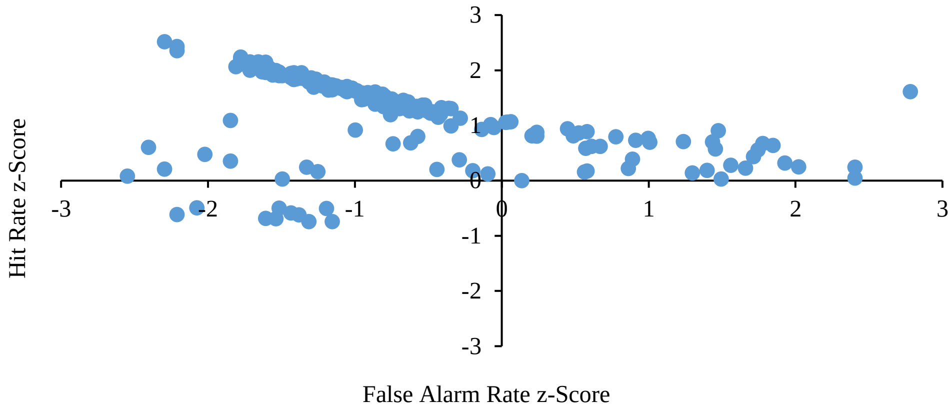

Figure 11 zROC plots for fall detection

4. Discussions

This study explores the effects of motion sensors (accelerometer and gyroscope) and ANN factors (hidden layer, epoch, number of neuron, learning rate, training function, and transfer function) on SDT outcomes (hit, miss, false alarm, correct rejection, A', $B"$, and zROC plot) for designing fall detection algorithm on wearable device. It has been found that the transfer function is significantly influenced the hit, miss, A', and $B"$. A better classification performance is achieved when a fall detection algorithm utilizes the RBF rather than the HTG [63] as it the RBF can show non-linear relations between input and output data [64] and be able to implement for multidimensional data [65]. These agree with the previous research findings [66-68] indicating that RBF has a better ability to classify the problem than the HTG.

Training function has influenced all SDT outcomes. The SCG becomes a robust training algorithm due to its minimum error corresponding to prior publications [69, 70] since it uses the Levenberg-Marquardt method in each iteration to avoid the line search in scaling the step size. For the improvement of fall detection performance, the FFANN trained with the SCG algorithm have been applied for resolving large-scale problems [71].

As found in the previous publication [23], the smaller number of neurons result in a greater A' providing a high classification accuracy and leading to a better detection performance (high hit and low false alarm rates). It should be noted that the SCG with the RBF allows the highest hit rate, A', and lowest miss since the main effects of two factors (training function and transfer function) are highly significant influenced on the SDT outcomes ($p < 0.01$) and strong interactions among them are found [18]. Additionally, SCG and the RBF with all hidden layers produces the high hit and the low miss rates. The design of fall detection algorithm with a low complexity of computation is recognized when choosing smaller ANN at the lowest level of the number of hidden layer and neuron [53].

The higher performance of pattern recognition classification is recognized when low complexity and less run-time consumption are found [53]. The analysis of FFD shows that the optimal parameters of fall detection algorithm consist of accelerometer with one gyroscope, one hidden layer, 100 epochs, low level (k=1) of number of neurons, 1 learning rate, the SCG, and the RBF.

The results obtained from this study provide the highest accuracy of 96.33% as compared to previous studies [51, 72-74] using ANN, as shown in Table 4.

Table 4 Comparison of this study and previous studies using ANN

Reference	Accuracy (%)	Sensitivity (%)	Specificity (%)
[72]	80.66	56.82	85.47
[73]	84.14	83.33	84.18
[74]	95.48	69.39	99.56
[51]	81.40	81.80	81.00
This study	96.33	96.76	95.41

This algorithm can be implemented in a standard general-purpose microcontroller [75]. The finding of ANN reveals the wearable fall detection device incorporating with only one accelerometer and one gyroscope allows the accurate and reliable performance. In addition, minimizing electronic components leads to small size, lightweight property, ease of use, and lower power consumption being consistent with the previous publication [76].

The prediction points generally fall on the upper-left area of zROC plot. However, there are still many points in the right area implying the poor performance of remaining experimental runs. The design of fall detection algorithms should be thoroughly considered to find the best performance configurations [24, 77] where the traditional method of problem solving e.g. trial and error takes a long period of time [12] and does not systematically focus on optimal solution [13, 62]. The FFD allows identifying and quantifying each design factor and interaction between factor levels [25] impacting ANN performance [19] to determine the best parameters of ANN [62].

5. Conclusions

In this study, the FFD proves the statistical difference of factors based on SDT outcomes to design a comprehensive and robust fall detection algorithm with minimum miss and false alarm rates [42, 77]. Therefore, the proposed method can be applied to ANN in many applications.

Findings from this study can serve as a technical guide of systematic design for determining the optimal parameters in designing fall detection algorithm and saving time during product design and development phase of ANN. There are two major limitations that should be mentioned. Firstly, independent variables of motion sensors are derived from the SisFall dataset with the simulation of ADLs and falls performed by healthy subjects. In additional to this, all experiments of ADLs and falls are not conducted and investigated. Secondly, the proposed fall detection algorithm employs binary classification technique where all type of falls and ADLs are divided into only two classes (falls and ADLs). As such, the classification of types of falls and ADLs can be achieved by implementing a multi-class classification technique [78] and should be considered for the future work.

6. Acknowledgments

This research was funded by King Mongkut's University of Technology North Bangkok. Contract no. KMUTNB-61-GOV-C2-50.

7. References

[1] World Health Organization. Falls [Internet]. 2021 [updated 2021 Apr 26; cited 2022 Jan 18]. Available from: https://www.who.int/news-room/fact-sheets/detail/falls.
[2] Tinetti ME, Williams CS. Falls, Injuries Due to Falls, and the Risk of Admission to a Nursing Home. N Engl J Med. 1997;337(18):1279-84.
[3] Koch S. Healthy ageing supported by technology - a cross-disciplinary research challenge. Inform Health Soc Care. 2010;35(3-4):81-91.
[4] Er PV, Tan KK. Non-intrusive fall detection monitoring for the elderly based on fuzzy logic. Measurement. 2018;124:91-102.
[5] Pierleoni P, Belli A, Palma L, Pellegrini M, Pernini L, Valenti S. A High Reliability Wearable Device for Elderly Fall Detection. IEEE Sens J. 2015;15(8):4544-53.
[6] Pannurat N, Thiemjarus S, Nantajeewarawat E. A Hybrid Temporal Reasoning Framework for Fall Monitoring. IEEE Sens J. 2017;17(6):1749-59.
[7] Ganapathy K, Vaidehi V, Poorani D. Sensor based efficient decision making framework for remote healthcare. J Ambient Intell Smart Environ. 2015;7(4):461-81.
[8] Aziz O, Musngi M, Park EJ, Mori G, Robinovitch SN. A comparison of accuracy of fall detection algorithms (threshold-based vs. machine learning) using waist-mounted tri-axial accelerometer signals from a comprehensive set of falls and non-fall trials. Med Biol Eng Comput. 2017;55(1):45-55.
[9] Yuwono M, Moulton BD, Su SW, Celler BG, Nguyen HT. Unsupervised machine-learning method for improving the performance of ambulatory fall-detection systems. BioMed Eng OnLine. 2012;11:1-11.
[10] Sorvala A, Alasaarela E, Sorvoja H, Myllylä R. A two-threshold fall detection algorithm for reducing false alarms. In: 6th International Symposium on Medical Information and Communication Technology (ISMICT); 2012 Mar 25-29; La Jolla, USA. USA: IEEE; 2012. p. 1-4.
[11] Abbate S, Avvenuti M, Corsini P, Light J, Vecchio A. Monitoring of human movements for fall detection and activities recognition in elderly care using wireless sensor network: a survey. In: Merrett GV, Tan YK, editors. Wireless Sensor Networks: Application-Centric Design. Shanghai: InTech; 2010. p. 1-20.
[12] Zhang G, Patuwo BE, Hu MY. Forecasting with artificial neural networks:: The state of the art. Int J Forecast. 1998;14(1):35-62.
[13] Balestrassi PP, Popova E, Paiva AP, Marangon Lima JW. Design of experiments on neural network's training for nonlinear time series forecasting. Neurocomputing. 2009;72(4-6):1160-78.
[14] Mahdi SQ, Gharghan SK, Hasan MA. FPGA-Based neural network for accurate distance estimation of elderly falls using WSN in an indoor environment. Measurement. 2021;167:108276.
[15] Wickens TD. Elementary signal detection theory. New York: Oxford University Press; 2002.
[16] Proctor RW, Van Zandt T. Human factors in simple and complex systems. Boston: Allyn & Bacon; 1993.
[17] Lin PH, Chen CH. Evaluating autostereoscopic 3D baseball games using signal detection theory and receiver operating characteristic space. Int J Ind Ergon. 2019;72:390-7.
[18] Montgomery DC. Design and analysis of experiments. 9th ed. New Jersey: John Wiley & Sons; 2017.
[19] Pontes FJ, Amorim GF, Balestrassi PP, Paiva AP, Ferreira JR. Design of experiments and focused grid search for neural network parameter optimization. Neurocomputing. 2016;186:22-34.
[20] Gökler SH, Boran S. Prediction of demand for red blood cells using ridge regression, artificial neural network, and integrated taguchi-artificial neural network approach. Int J Ind Eng: Theory Appl Pract. 2022;29(1):64-77.
[21] Lujan-Moreno GA, Howard PR, Rojas OG, Montgomery DC. Design of experiments and response surface methodology to tune machine learning hyperparameters, with a random forest case-study. Expert Syst Appl. 2018;109:195-205.
[22] Moreira MO, Balestrassi PP, Paiva AP, Ribeiro PF, Bonatto BD. Design of experiments using artificial neural network ensemble for photovoltaic generation forecasting. Renewable Sustainable Energy Rev. 2021;135:110450.
[23] Santos MS, Ludermir TB. Using factorial design to optimize neural networks. International Conference on Neural Networks; 1999 Jul 10-16; Washington, USA. USA: IEEE; 1999. p. 857-61.
[24] Nukala BT, Shibuya N, Rodriguez A, Tsay J, Lopez J, Nguyen T, et al. An efficient and robust fall detection system using wireless gait analysis sensor with artificial neural network (ANN) and support vector machine (SVM) algorithms. Open J. Appl. Biosens. 2014;3(4):29-39.
[25] Wang HK, Wang ZH, Wang MC. Using the Taguchi method for optimization of the powder metallurgy forming process for Industry 3.5. Comput Ind Eng. 2020;148:106635.
[26] Kaur P, Wang Q, Shi W. Fall detection from audios with Audio Transformers. Smart Health. 2022;26:100340.
[27] Xu T, Se H, Liu J. A fusion fall detection algorithm combining threshold-based method and convolutional neural network. Microprocess Microsyst. 2021;82:103828.
[28] Sucerquia A, López JD, Vargas-Bonilla JF. SisFall: a fall and movement dataset. Sensors. 2017;17(1):198.
[29] Luna-Perejón F, Domínguez-Morales MJ, Civit-Balcells A. Wearable fall detector using recurrent neural networks. Sensors. 2019;19(22):4885.

[30] Musci M, De Martini D, Blago N, Facchinetti T, Piastra M. Online fall detection using recurrent neural networks. arXiv:1804.04976. 2018:1-6.
[31] Waheed M, Afzal H, Mehmood K. Nt-fds—a noise tolerant fall detection system using deep learning on wearable devices. Sensors. 2021;21(6):1-26.
[32] Yu X, Koo B, Jang J, Kim Y, Xiong S. A comprehensive comparison of accuracy and practicality of different types of algorithms for pre-impact fall detection using both young and old adults. Measurement. 2022;201:111785.
[33] Noury N, Rumeau P, Bourke AK, ÓLaighin G, Lundy JE. A proposal for the classification and evaluation of fall detectors. IRBM. 2008;29(6):340-9.
[34] Wang G, Li Q, Wang L, Zhang Y, Liu Z. Elderly fall detection with an accelerometer using lightweight neural networks. Electronics. 2019;8(11):1354.
[35] Casilari E, Santoyo-Ramón JA, Cano-García JM. Analysis of public datasets for wearable fall detection systems. Sensors. 2017;17(7):1513.
[36] Hosseinian SM, Zhu Y, Mehta RK, Erraguntla M, Lawley MA. Static and dynamic work activity classification from a single accelerometer: implications for ergonomic assessment of manual handling tasks. IISE Trans Occup Ergon Hum Factors. 2019;7(1):59-68.
[37] Kangas M, Vikman I, Wiklander J, Lindgren P, Nyberg L, Jämsä T. Sensitivity and specificity of fall detection in people aged 40 years and over. Gait Posture. 2009;29(4):571-4.
[38] Lees MN, Lee JD. The influence of distraction and driving context on driver response to imperfect collision warning systems. Ergonomics. 2007;50(8):1264-86.
[39] Moon H, Han SH, Chun J. Applying signal detection theory to determine the ringtone volume of a mobile phone under ambient noise. Int J Ind Ergon. 2015;47:117-23.
[40] Huang YY, Menozzi M, Favey C. A screening tool for occupations requiring a high level of attentional performance. Int J Ind Ergon. 2019;72:86-92.
[41] Jiang X, Khasawneh MT, Master R, Bowling SR, Gramopadhye AK, Melloy BJ, at al. Measurement of human trust in a hybrid inspection system based on signal detection theory measures. Int J Ind Ergon. 2004;34(5):407-19.
[42] Liang SFM, Menozzi M, Huang YYR. A mechanism based on finger-sliding behavior for designing radial menus. Int J Ind Ergon. 2019;74:102869.
[43] Liu CL. Countering the loss of extended vigilance in supervisory control using a fuzzy logic model. Int J Ind Ergon. 2009;39(6):924-33.
[44] Michel S, Mendes M, de Ruiter JC, Koomen GCM, Schwaninger A. Increasing X-ray image interpretation competency of cargo security screeners. Int J Ind Ergon. 2014;44(4):551-60.
[45] Seong Y, Nam CS. Capturing judgment policy on customers' creditworthiness: a lens model and SDT approach. Int J Ind Ergon. 2008;38(7-8):593-600.
[46] Grier JB. Nonparametric indexes for sensitivity and bias: Computing formulas. Psychol Bull. 1971;75(6):424-9.
[47] Edgar GK, Catherwood D, Baker S, Sallis G, Bertels M, Edgar HE, et al. Quantitative analysis of situation awareness (QASA): modelling and measuring situation awareness using signal detection theory. Ergonomics. 2018;61(6):762-77.
[48] Stanislaw H. Calculation of signal detection theory measures. Behav Res Meth Instrum Comput. 1999;31:137-49.
[49] Lim S, D'Souza C. A narrative review on contemporary and emerging uses of inertial sensing in occupational ergonomics. Int J Ind Ergon. 2020;76:102937.
[50] Tausendschön J, Radl S. Deep neural network-based heat radiation modelling between particles and between walls and particles. Int J Heat Mass Transf. 2021;177:121557.
[51] Abbate S, Avvenuti M, Bonatesta F, Cola G, Corsini P, Vecchio A. A smartphone-based fall detection system. Pervasive Mob Comput. 2012;8(6):883-99.
[52] Gharghan SK, Mohammed SL, Al-Naji A, Abu-AlShaeer MJ, Jawad HM, Jawad AM, et al. Accurate fall detection and localization for elderly people based on neural network and energy-efficient wireless sensor network. Energies. 2018;11(11):2866.
[53] Munadhil Z, Gharghan SK, Mutlag AH, Al-Naji A, Chahl J. Neural Network-Based Alzheimer's Patient Localization for Wireless Sensor Network in an Indoor Environment. IEEE Access. 2020;8:150527-38.
[54] Shrestha SB, Song Q. Adaptive learning rate of SpikeProp based on weight convergence analysis. Neural Networks. 2015;63:185-98.
[55] Al-Majidi SD, Abbod MF, Al-Raweshidy HS. A particle swarm optimisation-trained feedforward neural network for predicting the maximum power point of a photovoltaic array. Eng Appl Artif. Intell. 2020;92:103688.
[56] Cameron R, Zuo Z, Sexton G, Yang L. A fall detection/recognition system and an empirical study of gradient-based feature extraction approaches. In: Chao F, Schockaert S, Zhang Q, editor. Advances in Computational Intelligence Systems. UKCI 2017. Advances in Intelligent Systems and Computing Volume 650. Cham: Springer; 2018. p. 276-89.
[57] Chernbumroong S, Cang S, Atkins A, Yu H. Elderly activities recognition and classification for applications in assisted living. Expert Syst Appl. 2013;40(5):1662-74.
[58] Xiao WB, Nazario G, Wu HM, Zhang HM, Cheng F. A neural network based computational model to predict the output power of different types of photovoltaic cells. PLoS One 2017;12(9):e0184561.
[59] Mittal M, Bora B, Saxena S, Gaur AM. Performance prediction of PV module using electrical equivalent model and artificial neural network. Sol Energy. 2018;176:104-17.
[60] Armstrong RA, Eperjesi F, Gilmartin B. The application of analysis of variance (ANOVA) to different experimental designs in optometry. Ophthalmic Physiol Opt. 2002;22(3):248-56.
[61] Smalheiser NR. ANOVA. In: Smalheiser NR, editor. Data literacy: how to make your experiments robust and reproducible. London: Academic Press; 2017. p. 149-55.
[62] Packianather MS, Drake PR, Rowlands H. Optimizing the parameters of multilayered feedforward neural networks through Taguchi design of experiments. Qual Reliab Eng Int. 2000;16(6):461-73.
[63] Gibson RM, Amira A, Ramzan N, Casaseca-De-La-Higuera P, Pervez Z. Multiple comparator classifier framework for accelerometer-based fall detection and diagnostic. Appl Soft Comput. 2016;39:94-103.

[64] Mustafa MR, Rezaur RB, Rahardjo H, Isa MH. Prediction of pore-water pressure using radial basis function neural network. Eng Geol. 2012;135-136:40-7.
[65] Mustafa MR, Isa MH, Rezaur RB. A comparison of artificial neural networks for prediction of suspended sediment discharge in river-a case study in Malaysia. World Acad Sci Eng Technol. 2011;81:372-6.
[66] Khosravi A, Koury RNN, Machado L, Pabon JJG. Prediction of hourly solar radiation in Abu Musa Island using machine learning algorithms. J Clean Prod. 2018;176:63-75.
[67] Vaziri N, Hojabri A, Erfani A, Monsefi M, Nilforooshan B. Critical heat flux prediction by using radial basis function and multilayer perceptron neural networks: a comparison study. Nucl Eng Des. 2007;237(4):377-85.
[68] Yilmaz AS, Özer Z. Pitch angle control in wind turbines above the rated wind speed by multi-layer perceptron and radial basis function neural networks. Expert Syst Appl. 2009;36(6):9767-75.
[69] Huda ASN, Taib S. Suitable features selection for monitoring thermal condition of electrical equipment using infrared thermography. Infrared Phys Technol. 2013;61:184-91.
[70] Rezaeian-Zadeh M, Tabari H, Abghari H. Prediction of monthly discharge volume by different artificial neural network algorithms in semi-arid regions. Arab J Geosci. 2013;6:2529-37.
[71] Møller MF. A scaled conjugate gradient algorithm for fast supervised learning. Neural Networks. 1993;6(4):525-33.
[72] Villar JR, Chira C, de la Cal E, González VM, Sedano J, Khojasteh SB. Autonomous on-wrist acceleration-based fall detection systems: unsolved challenges. Neurocomputing. 2021;452:404-13.
[73] Khojasteh SB, Villar JR, Chira C, González VM, de la Cal E. Improving fall detection using an on-wrist wearable accelerometer. Sensors (Basel). 2018;18(5):1-28.
[74] Martínez-Villaseñor L, Ponce H, Brieva J, Moya-Albor E, Núñez-Martínez J, Peñafort-Asturiano C. Up-fall detection dataset: a multimodal approach. Sensors. 2019;19(9):1988.
[75] Naranjo-Hernández D, Reina-Tosina J, Roa LM. Special issue “Body sensors networks for e-health applications”. Sensors. 2020;20(14):1-7.
[76] Al-Rakhami MS, Gumaei A, Altaf M, Hassan MM, Alkhamees BF, Muhammad K, et al. FallDeF5: A fall detection framework using 5G-based deep gated recurrent unit networks. IEEE Access. 2021;9:94299-308.
[77] Mubashir M, Shao L, Seed L. A survey on fall detection: Principles and approaches. Neurocomputing. 2013;100:144-52.
[78] Putra IPES, Brusey J, Gaura E, Vesilo R. An event-triggered machine learning approach for accelerometer-based fall detection. Sensors. 2018;18(1):1-18.